

Estimating uncertainty caused by ocean heat transport to the North Sea: experiments downscaling EC-Earth

T. Tian¹ · J. Su² · F. Boberg¹ · S. Yang¹ · T. Schmith¹

Received: 8 June 2014 / Accepted: 16 March 2015 / Published online: 31 March 2015
© Springer-Verlag Berlin Heidelberg 2015

Abstract The heat content of the North Sea is determined by the surface heat flux and the ocean heat transport into the region. The uncertainty in the projected warming in the North Sea caused by ocean heat transport has rarely been quantified. The difference in the estimates using regional ocean models is known to arise from the poorly prescribed temperature boundary forcing, either provided by global models at coarse grid resolutions, or from anomaly correction (using difference of the simulation from observed climatology) without interannual variation. In this study, two marine downscaling experiments were performed using boundary temperature forcings prepared with the two above mentioned strategies: one interpolated from a global model simulation (MI: model incl. interannual variation), and the other from observed climatology with warming trends in the future ocean derived from the global model simulation (OT: observed climatol. plus trend). The comparative experiments allowed us to estimate the uncertainty caused by ocean heat transport to the North Sea. The global climate model EC-Earth CMIP5 simulations of historical and future scenarios were used to provide lateral boundary forcing for regional models. The OT boundary was found to affect deep water temperatures (below 50 m) in the North Sea because of reduced interannual variability. The difference of mean temperature changes by 2100 (MI – OT) was up to 0.5 °C near the bottom across 58°N. While the

deep water temperature in the North Sea did not directly link to the large-scale atmospheric circulation, the Norwegian outflow was highly correlated with the NAO index and heat transport of the Atlantic inflow provided by EC-Earth. It was found that model uncertainty due to the choice of lateral boundary forcing could be significant in the interannual variation of thermal stratification in the northern North Sea in a long-term simulation.

Keywords EC-Earth · North Sea · Ocean heat transport · Ocean volume transport · Climate change · Marine downscaling

1 Introduction

Exchange of water mass properties between the northern North Sea and the adjoining North Atlantic Ocean is the principal driver, besides atmospheric forcing and river runoff, determining the circulation in the North and Baltic Seas. Therefore, this exchange determines to large parts any future climate changes in these regional seas (Otto et al. 1990; Turrell et al. 1996; Winther and Johannessen 2006; Holt et al. 2010). Investigations of such future hydrographic changes of the North and Baltic Seas with respect to the present day using dynamic downscaling have been developed over the last two decades (Meier 2006; Ådlandsvik and Bentsen 2007; Ådlandsvik 2008). Marine downscaling of a coarse-grid global model simulation is shown not only to provide regional details but also to enhance the Atlantic inflow to the North Sea and to increase the mean winter temperature (Ådlandsvik and Bentsen 2007). One of the challenges in these studies is to minimise the effect of the biased boundary values from a coarse-grid global model to the North Sea (Ådlandsvik and Bentsen 2007;

✉ T. Tian
tian@dmi.dk

¹ Danish Meteorological Institute, Lyngbyvej 100,
2100 Copenhagen, Denmark

² Institute of Oceanography, University of Hamburg,
Bundesstr. 53, 20146 Hamburg, Germany

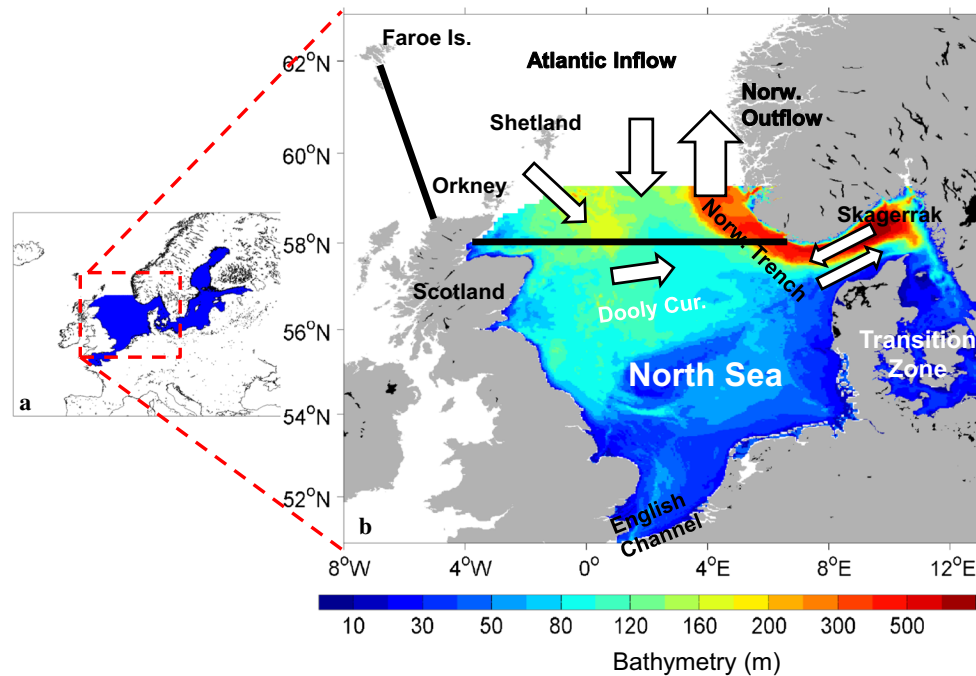


Fig. 1 **a** Regional ocean model domains for the North and Baltic Seas (filled in blue). The dashed lines delimit the region of interest. **b** Schematic diagram of the general circulation in the northern North Sea as well as the Atlantic inflow and the Norwegian outflow at the

northern North Sea boundary. The width of arrows is indicative of the relative magnitude of volume transport. The two black lines represent the Faroes–Scotland section and the 58°N section, respectively.

Ådlandsvik 2008; Holt et al. 2010). The global model often has non-negligible biases for the region of interest. A conventional way is to apply a bias correction with observed climatology (Mathis et al. 2013). However, this method may introduce a large uncertainty when simulating the future marine climate due to the absence of time-varying information. The bias in estimating ocean heat transport to the North Sea can arise either inherited from the global model of poor spatial resolution, or from missing temporal variation in mean annual cycle compiled from multi-year observations. Its effect on temperature changes in marine downscaling of future climate scenarios for the North Sea has rarely been quantified.

The Atlantic water enters the North Sea mainly from the north through the Shetland–Orkney section, the Shetland shelf area and the western part of the Norwegian Trench, with only <10 % of water entering from the English Channel (Fig. 1). The only exit is along the Norwegian coast. The overall long-term mean circulation pattern in the North Sea exhibits a cyclonic circulation along its periphery (Turrell et al. 1996). Water exchange between the North and Baltic Seas is controlled by the salinity difference between the North Sea and the brackish Baltic Sea and by the vertical mixing in the stratified transition zone (Fig. 1b).

At the northern North Sea boundary (Fig. 1), the inflow in the deep trench reaches the inner part of

Skagerrak, meets brackish water from the Baltic and turns northwards, leaving the North Sea along the Norwegian coast. The inflow in the Shetland–Orkney section has a major pathway eastward and crosses the central North Sea along the 100 m isobath, known as the Dooley Current (Dooley 1974; Svendsen et al. 1991). The seasonal and interannual variation in oceanic transport determines the composition of inflowing water. This variation may affect the magnitude of the circulation within the North Sea through density effects, the nutrient from the warm Atlantic water entering the North Sea, and the transport of oceanic plankton into the North Sea (Turrell et al. 1996).

Observations (Orvik and Skagseth 2005) indicated that the interannual and decadal variations of the Atlantic inflows to the Norwegian Sea and the North Sea were strongly connected to large-scale atmospheric patterns like the North Atlantic Oscillation (NAO). Numerical studies by Winther and Johannessen (2006) showed that the relation between the NAO index and the North Sea fluxes varied with time and location. The inflow in the Norwegian Trench has a longer response time to NAO than the inflow in the Shetland–Orkney section and the Shetland shelf area. Although the modelling study by Hjøllo et al. (2009) suggested a minor effect of advective fluxes on heat content in the North Sea from 1985 to 2007, an open question is, how

strongly the North Sea heat and volume fluxes are coupled to the NAO index under climate warming.

The present study analyses variability and changes of temperature in the North and Baltic Seas, as simulated by a regional ocean model driven with two kinds of temperature boundary forcings. Our first regional downscaling experiment, referred to as experiment MI hereafter, applies boundary forcing interpolated from transient climate simulations by EC-Earth for the period 1960–2100. The another comparative downscaling experiment, referred to as OT hereafter, is forced with observed climatology plus a linear warming trend derived from the above mentioned EC-Earth simulations. The comparison provides a reference, to some extent, about the uncertainty in dynamic downscaling induced by lateral ocean temperature boundary forcing. The two numerical experiments are used to investigate boundary effects on thermal stratification, advective heat flux and volume transport in the North Sea. Particularly, we seek to investigate the connection of NAO and the Atlantic inflow to lateral heat transport into the North Sea in winter. The influence of the inflow at the English Channel is not considered in this paper, not only because changes in heat flux do not affect the stratification due to strongly tidal mixing in this region (Holt et al. 2010), but also because its inflow is relatively weak in winter compared to the inflow at the northern North Sea boundary (Winther and Johannessen 2006).

The study is organized as follows. After this introduction, the regional ocean model and the downscaling experiments with two different ocean boundary forcings as well as data from the EC-Earth simulations are described. Section 3 presents the results from the model simulations, starting with an analysis of the EC-Earth forcing data followed by more detailed analyses on temperature changes, ocean volume and heat transports in the North Sea. Section 4 discusses model uncertainty in the projected warming in the North Sea and the connection with NAO. Section 5 provides conclusions from this study. In the “Appendix” section, description about the regional atmospheric forcing for the ocean model and the preparation for the ocean boundary data are provided.

2 Data and methodology

2.1 The EC-Earth CMIP5 simulations

EC-Earth is a global coupled climate model. Its atmospheric component is the Integrated Forecast System (IFS) of the European Centre for Medium Range Weather Forecasts (ECMWF) while its ocean component is the Nucleus for European Modelling of the Ocean (NEMO) developed by Institut Pierre et Simon Laplace (IPSL) with the

Louvain-la-Neuve sea Ice Model (LIM) embedded (Hazeleger et al. 2012). The atmospheric and ocean modules are coupled by the OASIS3 coupler. The details of model configuration and performance are described in Hazeleger et al. (2012). The EC-Earth simulations used here are following the fifth phase of Coupled Model Intercomparison Project (CMIP5) protocol (Taylor et al. 2012) and NEMO is configured with the ORCA1 tri-polar nominal 1° grids. The historical experiment, initialized from a selected year of a control run, used time-varying historical forcing (i.e. solar forcing, GHGs, ozone, man-made and volcanic aerosol concentrations and historical land-use) starting in 1850 and ending in 2005. The ocean and atmospheric circulations develop according to the model internal dynamics and physics with no other constraints. The future experiments started following the historical run from 2006 and continued to 2100 with stipulated time-development of the aforementioned climate forcings according to the scenarios RCP4.5 and RCP8.5 (Vuuren et al. 2011).

NAO indices and heat transport of the Atlantic inflow were both calculated for winter from the EC-Earth simulations for the baseline (historical) period 1960–2009 and the scenario period 2010–2100. The NAO index was determined by the difference of the normalized mean sea level pressure (MSL) between two regional averages, i.e. (90°W – 60°E , 20°N – 55°N) – (90°W – 60°E , 55°N – 90°N), with respect to the base line period (see Stephenson et al. 2006). Heat transport of the Atlantic inflow was calculated for the section between Faroes (61.74°N , 6.74°W) and Scotland (58.62°N , 5.4°W) from the surface to 500 m’s depth (see Fig. 1b).

2.2 The regional ocean model

The regional ocean model used in this study is the HIROMB-BOOS-Model (HBM) (Berg 2012). HBM is a 3D, baroclinic circulation model that uses the hydrostatic and Boussinesq assumptions. The primitive equations are discretized on an Arakawa C-grid. The mixing scheme applied is based on the $k - \omega$ turbulence model (Umlauf et al. 2003). The model for the North Sea–Baltic Sea has a horizontal resolution of 6 nm (eddy resolving) and a maximum of 50 vertical layers with a thickness of 8 m in the surface layer (to avoid drying at low tides) and 2 m between the depths of 8 and 80 m. Below 80 m, the layer thickness increases gradually from 4 to 50 m. The model is set up horizontally in spherical coordinates and vertically in z coordinates. It has also a nested fine model for the transition area (at 1 nm). The time steps of the coarse and fine model are 90 and 45 s, respectively. This model configuration has been adapted to climate simulations (Madsen 2009; Tian et al. 2013).

The downscaling simulation started from January 1, 1960 with the initial ocean conditions taken from a climate

simulation (Madsen 2009). The first 3 years until January 1, 1963 were considered as a spin-up period for the ocean circulation to adjust to the atmospheric forcing, leaving the 47 years 1963–2009 as the historical period. For reasons of convenience, we extended the historical period until 2009 using the RCP4.5, as suggested by CMIP5 (CMIP5 update 2010). The downscaling simulation continued from January 1, 2010 for the future period for the two scenarios, respectively.

The ocean model surface was forced by hourly output from the HIRHAM regional atmospheric model downscaling of the EC-Earth CMIP5 experiments (see “Appendix 1”). For the riverine freshwater input to the ocean model, a monthly climatology has been compiled from available observational data (Madsen 2009). This climatological freshwater input was applied throughout the simulation. No change has been

made for the scenario simulations, since the uncertainties of future runoff in the Baltic are large (BACC 2011).

At the open boundaries of the model, namely the northern North Sea (59.25°N) and the English Channel (4.08°W), the model was forced by the synoptic sea level, tides, lateral temperature and salinity fields as described in Sect. 2.3. The synoptic sea levels were calculated from a northeast Atlantic barotropic surge model (NOAmod), also driven by hourly output from HIRHAM. There are no density (steric) effects considered in NOAmod. The tides were determined from 17 major tidal constituents. A lateral sponge zone acted as a buffer zone between the inner model domain and the boundary values of temperature and salinity. The operation of HBM is documented in details by Berg (2012).

Table 1 List of acronyms for model runs

	Historical (1963–2009)	RCP4.5 (2010–2100)	RCP8.5 (2010–2100)
MI boundary (model incl. interannual variation)	MIHIS	MIR4	MIR8
OT boundary (observed climatology plus trend)	OTHIS	OTR4	OTR8

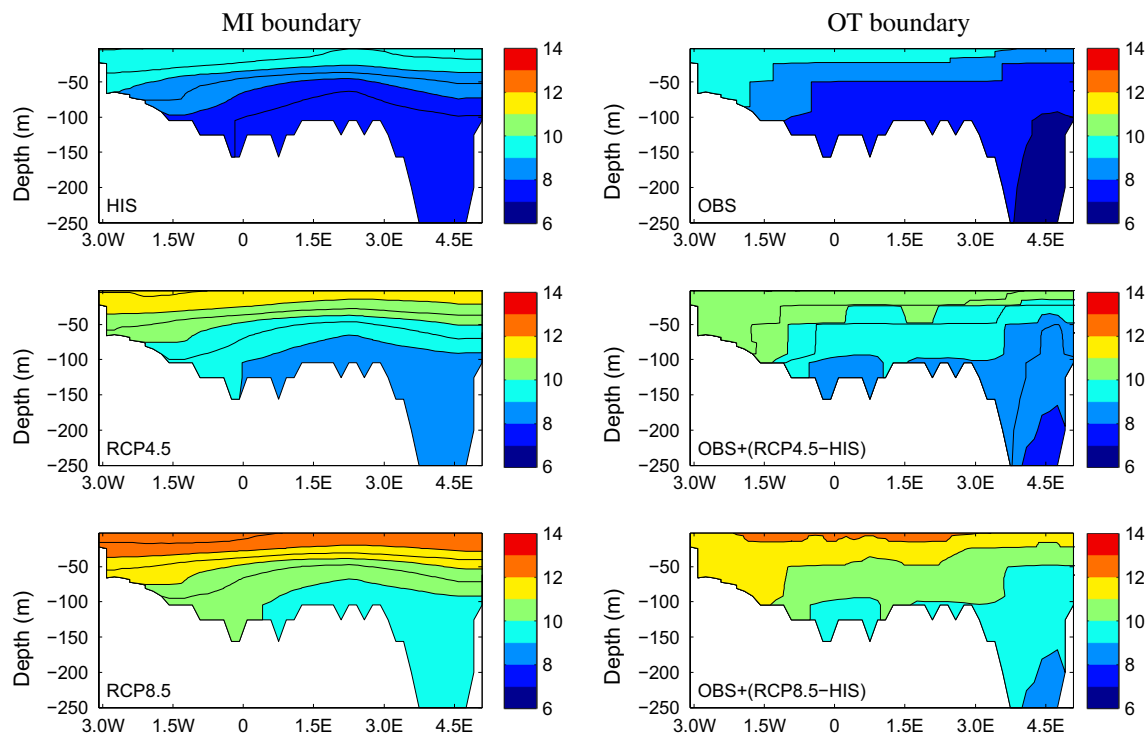


Fig. 2 30-year mean temperature over the historical period (1980–2009) and the future period (2071–2100) along the northern North Sea boundary (59.25°N). MI boundary: temperature is taken from EC-Earth including interannual variation. HIS, RCP4.5 and RCP8.5 represent climatology from the historical and future simulations for

the two scenarios, respectively. OT boundary: temperature is taken from observed climatology plus a warming trend in the future ocean derived from EC-Earth. OBS represents the ICES observational climatology; the future period climatology is calculated by OBS plus the differences between RCPs and HIS climatology

2.3 Ocean boundary forcing

As mentioned above, we prepared two sets of ocean temperatures as boundary forcings, MI and OT respectively (see Fig. 2). The MI (model incl. interannual variation) boundary was taken from monthly averages of the above EC-Earth simulations. The OT (observed climatol. plus trend) boundary for the historical period 1960–2009 was taken from the monthly climatology compiled by Jansen et al. (1999) from the ICES oceanographic observations (www.ices.dk). For the period 2010–2100, the OT boundary was obtained by taking the linear trend from the EC-Earth CMIP5 simulation and adding it to the ICES climatology described above. The details of boundary preparation are described in “Appendix 2”. Both OT and MI boundaries have their weaknesses and strengths: the MI boundary temperature resolves lateral heat transport in EC-Earth with interannual variations (incl. possible NAO-related variability), but shows some biases when compared to observed climatology (see Sect. 3.1); the OT boundary temperature includes both observed stratification and the EC-Earth simulated warming trends, but lacks interannual variations. The two different boundary temperatures were used for downscaling experiments in order to investigate their effects on future temperature change. The comparison between the two experiments was carried out for the two future scenarios. The acronyms for downscaling experiments are listed in Table 1.

The boundary salinity was taken from the ICES climatology for the period 1960–2009. The ICES climatology plus a projected linear trend from EC-Earth was defined as the boundary salinity for the period 2010–2100. This prescribed salinity forcing was used for all experiments because the EC-Earth simulated salinity is unrealistically high in the eastern side of surface water, e.g. salinity >34.4 in EC-Earth versus <33 in OBS (see Fig. 10 top panels). Furthermore, the comparison focused on the role of lateral heat transport. Hence, we used the same boundary salinity to eliminate the effect of salinity on density changes. The effect of salinity changes due to precipitation and freshwater discharge within the North and Baltic Seas was assumed negligible relative to the freshening trend in the open Atlantic (Jones and Howarth 1995).

3 Results

3.1 Temperature changes at the ocean boundary as simulated in EC-Earth

The vertical distribution of 30-year mean annual temperature at the northern North Sea boundary is shown in Fig. 2. In the historical simulation (Fig. 2, HIS), EC-Earth

is generally capable of reproducing the temperature in the surface and deep water obtained from the ICES observations (Fig. 2, OBS). However, it overestimates sea surface temperature (SST) in the eastern part of the boundary. Relative to the historical period of simulation (1980–2009), averaged temperature in the future period (2071–2100) increases by 1.6 °C in SST and 1.4 °C in the deep water under the RCP4.5 scenario (Fig. 2, RCP4.5 – HIS); and increases by 2.8 in SST and 2.4 °C in the deep water under the RCP8.5 scenario (Fig. 2, RCP8.5 – HIS). The maximal vertical gradient of temperature is 0.06 °Cm⁻¹ (HIS), 0.062 °Cm⁻¹ (RCP4.5) and 0.069 °Cm⁻¹ (RCP8.5), respectively.

The annual mean of SST and the deep water temperature (below 50 m) averaged along the northern North Sea boundary is shown in Fig. 3. The simulated climatology of the historical simulation (HIS, 1900–1999) is approximately 0.1 °C higher than the ICES climatology (OBS) of 9.2 °C in SST and 0.2 °C lower than OBS of 7.4 °C in the deep water. There is a clear warming trend in the EC-Earth simulated temperature under the RCP4.5 and RCP8.5 scenarios.

3.2 Temperature variability and advective heat flux in marine downscaling

Based on the downscaling simulations, the 30-year mean temperature over the period 1980–2009 is 8.7 °C in the North Sea (including the transition water) and 5.8 °C in

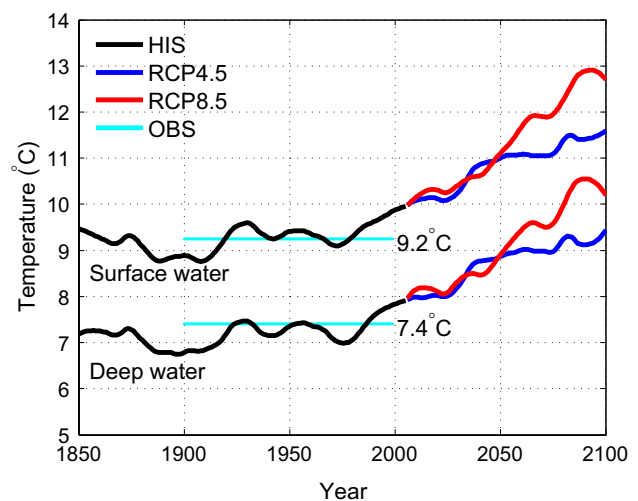


Fig. 3 Annual mean temperature of the sea surface water and the deep water below 50 m along the northern North Sea boundary from the historical period 1850–2005 (HIS, black lines) to the future period 2006–2100 under scenario RCP4.5 (dark blue lines) and RCP8.5 (red lines), projected by EC-Earth. The reference values of 9.2 and 7.4 °C are the ICES observational climatology 1900–1999 (OBS, light blue lines). For all time series, a loess (local polynomial regression fitting) smoother is applied (span = 0.12 with half-amplitude point centered on a 15-year period)

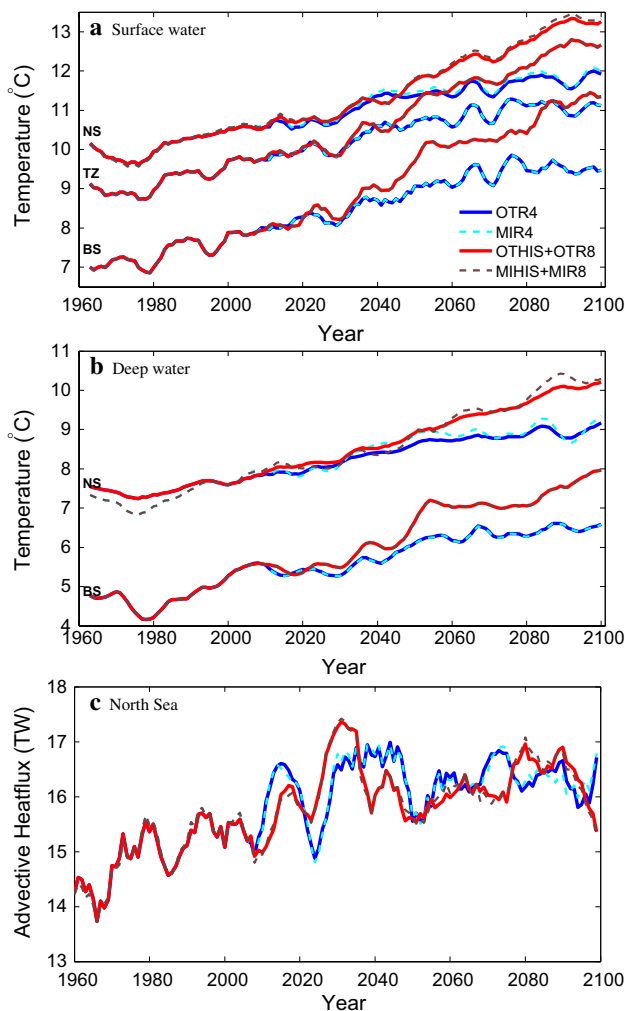


Fig. 4 **a, b** Annual mean of SST and deep water temperature averaged below 50 m in the North Sea (NS), the transition zone (TZ) and the Baltic Sea (BS). **c** Annual average of the advective heat flux into the North Sea. Data are taken from the OT (solid line) and MI (dashed line) experiments and are shown as 7-year moving averages. The acronyms for downsclaing experiments are listed in Table 1

the Baltic Sea (east of 13°E), while there is an increase of 2.5 °C in the North Sea and 2.7 °C in the Baltic Sea by the period 2071–2100 under RCP8.5 (not shown). The annual mean of SST and deep water temperature (below 50 m) show a general increase in the North and Baltic Seas (Fig. 4). The mean change of SST between the two time slices is 2.6, 2.9 and 3.3 °C in the North Sea (excluding Skagerrak), the transition water and the Baltic Sea, respectively (Fig. 4a). There is only 0.1 °C SST difference between the OT and MI experiments, reflecting a dominant role of atmospheric forcing, which is identical in the two experiments, in driving SSTs. The mean temperature change below 50 m is 2.5 °C in the North Sea and 2.4 °C in the Baltic Sea (Fig. 4b). The mean temperature below 50 m shows more interannual variability in the North Sea

in MI experiments than in OT experiments, with a difference below -0.5 °C in 1975 and above 0.4 °C in 2090 (MI – OT). Such a difference due to boundary effects is confined to the northern North Sea because the southern North Sea is generally shallower than 50 m (see Fig. 1b). The boundary effect in the northern North Sea vanishes along the transition zone between the North and Baltic Seas because of the shallowness. Therefore, we only focus on the boundary effect in the northern North Sea.

In Fig. 4c, advective heat flux into the North Sea was determined by subtracting the total surface heat flux from the change in total heat content of the North Sea. The magnitudes of the annual average of the advective heat flux in the late twenty-first century are comparable for the two RCP scenarios, suggesting a dominant contribution of surface heating to the warming of the North Sea. After detrending the time series of wintertime advective heat flux and mean temperature below 50 m (not shown), their correlations are slightly higher in MI experiments with 0.46 (MIR4) and 0.54 (MIR8) than in OT experiments with 0.44 (OTR4) and 0.52 (OTR8).

In order to display spatial variability of the boundary forcing effect on a seasonal scale, the mean temperature below 50 m was calculated as seasonal mean for each year for the scenario RCP8.5. The time series of seasonal mean at each grid point were further detrended and then used to calculate the standard deviation in the northern North Sea. The standard deviation near the northern North Sea boundary is associated with ocean boundary forcing, ocean circulation and water depth. Since there is no interannual variability in the OT boundary forcing after detrending, the difference of spatial pattern between DJF and JJA mean near the open boundary (shown as blue color in Fig. 5, OTR8) should be attributed to the difference between winter and summer in the ocean circulation. In comparison of seasonal mean between MIR8 and OTR8, the difference (i.e. MIR8 – OTR8) results from the interannual variability in MI boundary. The standard deviation difference between MIR8 and OTR8 is found to be larger than 0.2 °C near the northern North Sea boundary with water depth >100 m. Similar features are also found in the RCP4.5 scenario (not shown).

3.3 Temperature and volume transport across 58°N

By the end of the twenty-first century, temperatures along a section at 58°N (see Fig. 1b) increase over 1 and 2 °C under the scenario RCP4.5 and RCP8.5, respectively (Fig. 6). Temperatures below 50 m generally change more in MI simulations than in OT simulations, particularly in the scenario RCP8.5. Consistent with Fig. 5, temperature change near the bottom along the section indicates a strong seasonal signal, with warmer inflow in the shallow basin along the Shetland–Orkney section in February and in the deep trench in

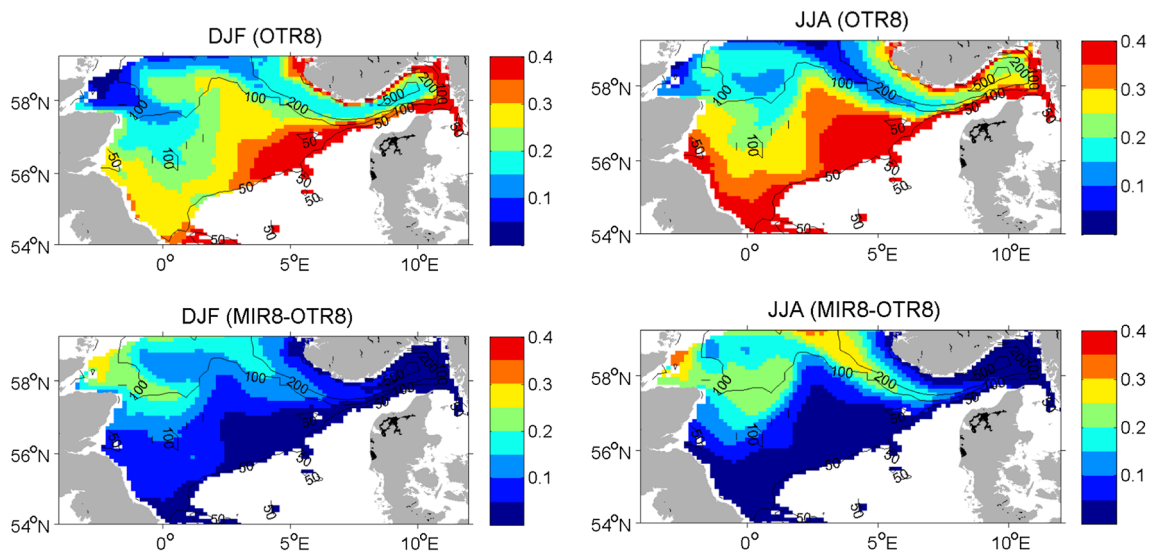


Fig. 5 Standard deviation of seasonal mean temperature below 50 m in DJF (*left*) and JJA (*right*) for the OTR8 experiment (*top panels*) and the standard deviation differences between the MIR8 and OTR8

August in MI simulations than in OT simulations. Between MI and OT simulations, the difference of mean temperature changes is up to 0.5 °C near the bottom, suggesting significant differences in thermal stratification caused by the different choice of boundary forcing in a long-term run.

To evaluate the influence of large-scale atmospheric circulation patterns, we analysed the relation between NAO, heat and volume transport into the North Sea in winter. Figure 7 plotted the mean temperature below 50 m, the EC-Earth simulated NAO index and ocean heat transport across the Faroes–Scotland section. It is evident that, while the correlation between ocean heat transport and the NAO index is high (i.e. 0.65), both of them have near-zero correlation with mean temperature below 50 m across 58°N (Fig. 7). We further show a Hovmöller Diagram of volume transport difference between MIR8 and OTR8 across 58° N, which covers the Shetland inflow in the west and the Norwegian outflow in the east (Fig. 8). The MI boundary results in more inflow through the Norwegian Trench (around 4°E) as well as more outflow of the Norwegian Coastal Current (around 6°E) in most years than the OT boundary. The wintertime difference is approximately <math><0.05\text{ Sv}</math> (the mean wintertime Norwegian outflow $\sim 1.3\text{ Sv}$ in Fig. 9). The Norwegian Coastal Current, which is an indicator of total ocean current out of the North Sea, shows a significant correlation with either the NAO index of 0.68 for OTR8 and 0.7 for MIR8, or ocean heat transport of 0.57 for OTR8 and 0.6 for MIR8 as indicated in Fig. 9. This suggests volume fluxes in (or out of) the North Sea highly associated with large-scale atmospheric patterns like NAO and the Atlantic inflow.

experiments (*bottom panels*). The temperature time series, taken from the scenario RCP8.5 simulation (2010–2100), are detrended. The acronyms for downscaling experiments are listed in Table 1

4 Discussion

4.1 Model uncertainty in marine temperature changes

The heat content of shelf seas like the North Sea is determined by surface heat flux and advective heat flux into the region of concern. The latter was shown to play a minor role in heat content in the North Sea by Hjøllø et al. (2009). Numerical experiments by Wakelin et al. (2009) showed that climatological boundary conditions are missing information on inter-annual variability that exists in the model simulations. This appeared to impact on both heat and volume transport in the deep water of the northern North Sea. Our experiments confirm this with exploration of decadal change, and further complement to this point by showing nearly no difference in heat content in the southern North Sea and the adjacent Baltic Sea between experiments forced with the two kinds of boundary forcings of MI and OT, respectively.

We investigate how advective heat fluxes from the adjoining deep ocean might influence the temperature and stratification of the northern North Sea in the late twenty-first century. Whether climatological lateral boundary values (e.g. OT) are adequate in marine downscaling for future projection is thus the key question in this paper. The basic assumptions behind the method are that the contribution of advective heat transport to the warming of the North Sea is minor relative to surface heat flux, and that model uncertainty induced by time-varying boundary information from global models (e.g. MI) is negligible (Mathis et al. 2013; Holt et al. 2010). Indeed, the mean temperature below

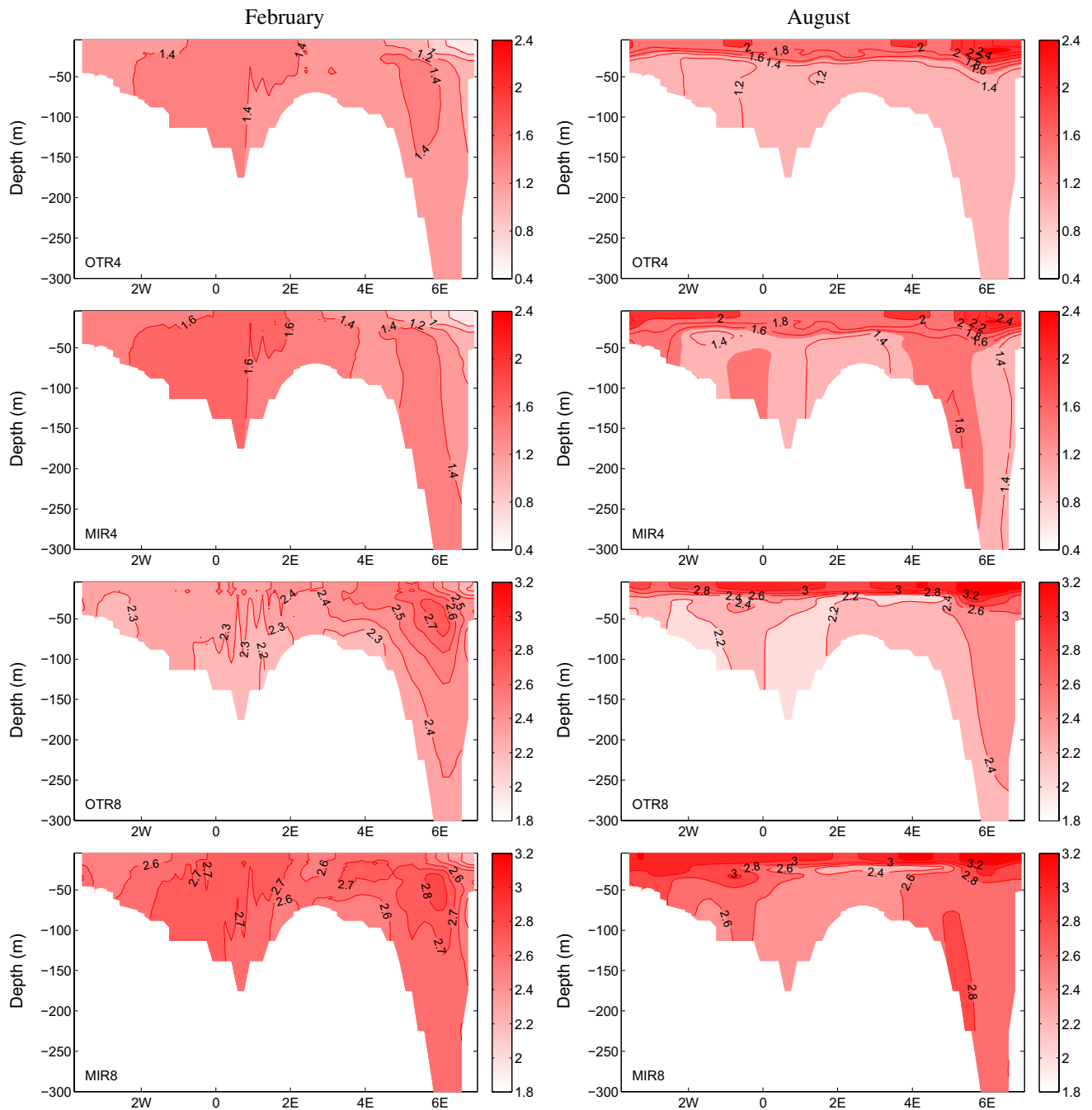


Fig. 6 20-year mean temperature change (i.e. 2080–2099 – 1986–2005) in February (*left*) and August (*right*) across 58°N for the scenario experiments driven with OT and MI. Note that the colorbars for the two scenarios are different

50 m demonstrates more interannual variability spatially and seasonally in MI experiments than in OT experiments (Fig. 5), and the temperature difference may reach 0.5 °C between MI and OT in some years (Fig. 4b). The correlation between advective heat flux and mean temperature below 50 m in MI experiments is also slightly higher than in OT experiments. Comparing the future and present time slices, temperatures below 50 m generally change more in

MI than in OT simulations (Fig. 6). The difference of mean temperature changes toward the end of the twenty-first century (i.e. MI – OT) is up to 0.5 °C near the bottom across 58°N, which is comparable to the observed temperature change of 0.62 °C in the last 20 years (Hjøllo et al. 2009). These results suggest that experiments driven by the climatological boundary conditions may seriously underestimate the interannual variation of thermal stratification, and

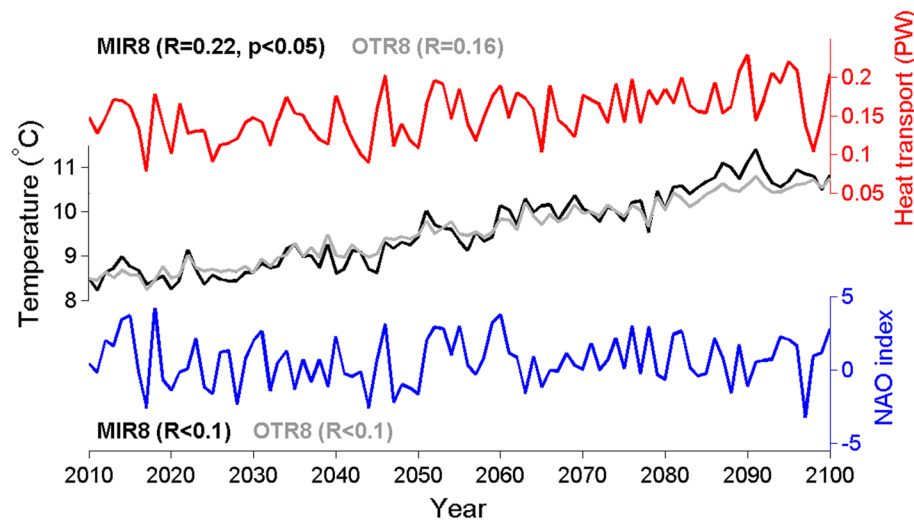


Fig. 7 Evolution of wintertime (DJF) mean temperature below 50 m across 58°N (black and grey lines), the NAO index (blue line) and ocean heat transport across the Faroes–Scotland section (red line) under the scenario RCP8.5. The NAO index and heat transport are calculated from the EC-Earth simulation and the correlation between

them is 0.65. Temperature is simulated in MIR8 (black line) and OTR8 (grey line). The correlations (R and p values) of mean temperature below 50 m to heat transport (NAO index) are calculated from the detrended time series and listed above (below) the corresponding time series

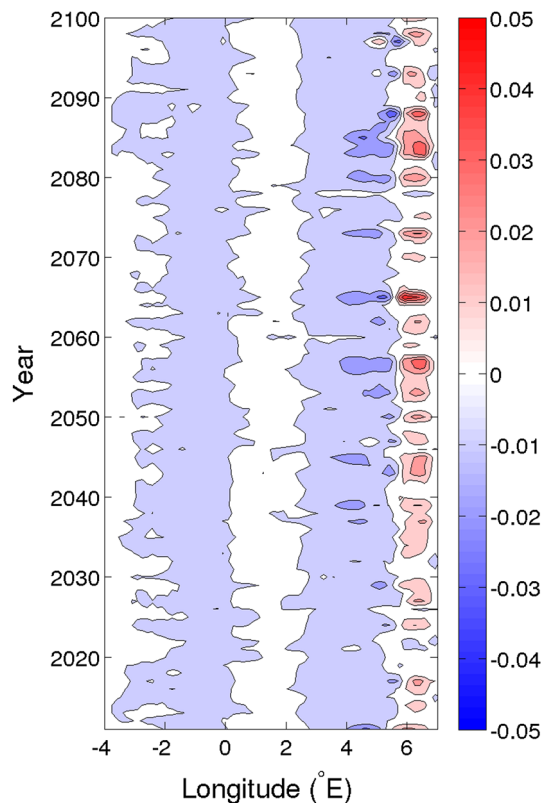


Fig. 8 Hovmöller Diagram of volume transport difference in Sv (MIR8 – OTR8) in wintertime (DJF) across 58°N. Blue (red) colors indicate more southward (northward) transport in MIR8, respectively

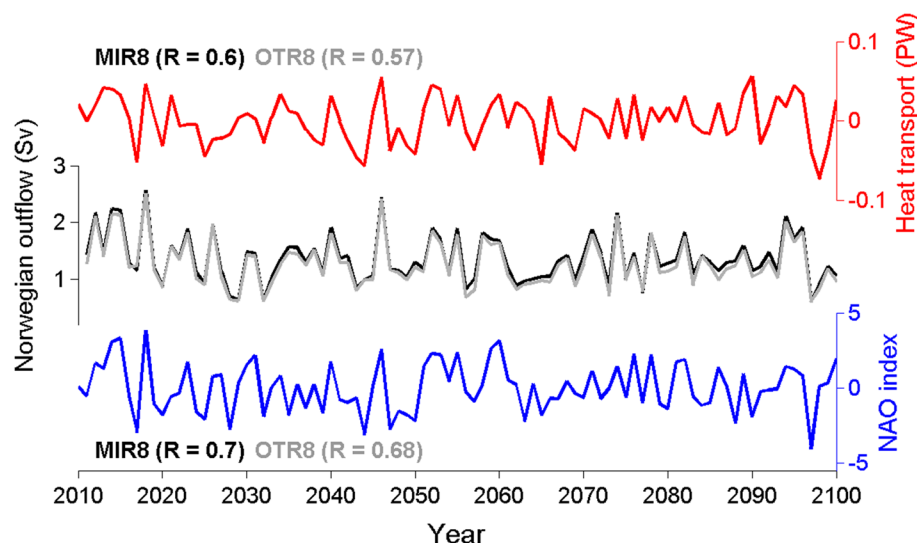
thereby affecting the basin-wide baroclinic circulation. The assessment may have important implication to many subjects, such as studies focused on extreme events, decadal variability and uncertainties in thermal stratification and marine ecology.

4.2 Connection with NAO in the global model EC-Earth

Many studies have demonstrated that the major influence of NAO in the North Sea in winter is on sea level, which in turn determines the volume flux of the Norwegian outflow (Yan et al. 2004; Tsimplis and Shaw 2008; Dangen-dorf et al. 2012). In our study, the volume flux of the Norwegian outflow has strong correlation with NAO ($R \sim 0.7$) and ocean heat transport across the Faroes–Scotland section ($R \sim 0.6$) in both MI and OT simulations (Fig. 9). The wintertime difference of volume flux (i.e. MI – OT) is relatively small, only 0.05 Sv compared to the winter mean Norwegian outflow of ~ 1.3 Sv (Figs. 8, 9). We conclude that neither OT nor MI boundaries will alter regional response to the general circulation pattern of NAO in the North Sea when downscaling. The uncertainty in volume transport caused by temperature lateral boundary is negligible.

There is no interactive coupling between the atmosphere and seas in this downscaling application, although regional interactive coupling was found to unlikely affect the large-scale atmospheric circulation (Tian et al.

Fig. 9 Evolution of winter-time (DJF) Norwegian outflow through 58°N (black and grey lines), the NAO index (blue line) and ocean heat transport across the Faroes–Scotland section (red line) under the scenario RCP8.5. The NAO index and heat transport are calculated from the EC-Earth simulation and both time series are detrended. Outflow is simulated in MIR8 (black line) and OTR8 (grey line). The correlations of the Norwegian outflow to heat transport (NAO index) are all significant with $p < 0.001$ and listed above (below) the corresponding time series



2013), such as NAO. The current uncoupled configuration leads to the dominant role of surface atmospheric forcing in shallow waters like the southern North Sea and the North-Baltic Sea transition (Fig. 4a, b). Changes in advective heat flux showed little impact on temperature changes in these regions. The potential for anomalous advective heat flux to introduce temperature anomaly and in turn influence stratification in deep waters will be explored with a coupled regional climate model in the future study.

5 Conclusions

In this study, we investigated uncertainty caused by different constraints on ocean heat transport to the North and Baltic Seas applied for marine downscaling from the global model EC-Earth simulation for the present day and two future scenarios RCP4.5 and RCP8.5. The downscaling strategy with MI and OT lateral boundary forcings in this study may also be applied to other global models. The OT boundary was found to significantly affect deep water temperatures in the northern North Sea because of reduced interannual variability. Between MI and OT experiments, the difference of mean temperature changes at the end of the twenty-first century under the scenario RCP8.5 is up to 0.5 °C across 58°N, whereas it had little impact on temperature changes in the southern North Sea and the Baltic Sea because of the dominant role of surface atmospheric forcing in the upper North Sea and the transition area in uncoupled downscaling experiments. Our analysis throughout the downscaling simulation period 1960–2100 showed that lateral heat transport could cause changes in interannual variability in thermal stratification and water transport in the North Sea. The temperature changes below 50 m were

associated more with advective heat flux in MI experiments than in OT experiments, but it had no correlation with the NAO index nor with ocean heat transport across the Faroes and Scotland section simulated by EC-Earth. However, the Norwegian outflow was highly correlated with NAO and ocean heat transport in both OT and MI simulations, with only small difference between MI and OT. We conclude that model uncertainty caused by ocean heat transport to the North Sea could be significant in the interannual variation of thermal stratification, but its effect on volume transport is negligible in a long-term simulation.

Acknowledgments The present work received financial support from the Danish Strategic Research Council through its support of the Centre for Regional Change in the Earth System (CRES; www.cres-centre.dk) under Contract No. DSF-EnMi 09-066868 and furthermore it is part of the Greenland Climate Research Centre (Project 6504). The first author also received financial support from the Baltadap project (EU INTERREG IV B project). The authors thank Kristine S. Madsen for her early contribution to the climate modelling work and Jacob Woge Nielsen for comments during the process. We are grateful to two anonymous reviewers for their constructive comments, which improved our manuscript.

Appendix 1: Regional climate downscaling

The EC-Earth simulations were used to provide lateral boundary forcing and SST fields for the regional atmospheric model HIRHAM (Christensen et al. 2006). Dynamical downscaling was performed at a horizontal resolution of 6 nm with 31 vertical levels. The zonal and meridional wind components, temperature and specific humidity at all atmospheric model levels as well as surface pressure fields were introduced to HIRHAM as forcing at the lateral

boundaries at 6-h intervals. SST fields were interpolated and prescribed to HIRHAM once per day.

HIRHAM has been extensively used over the European region to downscale variability and climate change signals from the global model, for instance during the PRUDENCE projects (Christensen and Christensen 2007). In the present study, HIRHAM provided hourly surface forcing of 10 m wind, 2 m air temperature, mean sea level pressure, specific humidity and cloud cover for the regional ocean model HBM. Both models were set to the same horizontal model grid. This configuration has been validated with 20-year hindcast experiments (Tian et al. 2013).

Appendix 2: Open ocean boundary forcing

The MI and OT boundary forcings of temperature were used in downscaling experiments. The acronyms for downscaling experiments were listed in Table 1.

The MI forcing was obtained by interpolating the monthly temperatures from the EC-Earth simulations in space and time. The northern North Sea boundary (58.0°N–59.5°N, 3.0°W–6.0°E) and the western part of the English Channel boundary (48.0–50.5°N, 3.5–4.5°W) were defined to extract the gridded temperature and salinity values from the EC-Earth simulations.

To prepare the OT forcing of temperature, the ICES monthly climatology was taken for the historical period 1960–2009. For the period 2010–2100, a linear trend was first calculated between the climatology of the historical period 1980–2009 and the future period 2071–2100 based on the EC-Earth simulations. This linear trend plus the ICES historical climatology was then defined as the boundary forcing for the period 2010–2100. Using this method, the OT boundary forcing can both include the seasonality of the observed climatology and the warming trends in EC-Earth (Fig. 2). The same method was applied for salinity. The OT forcing of salinity was then used in all experiments (see Fig. 10).

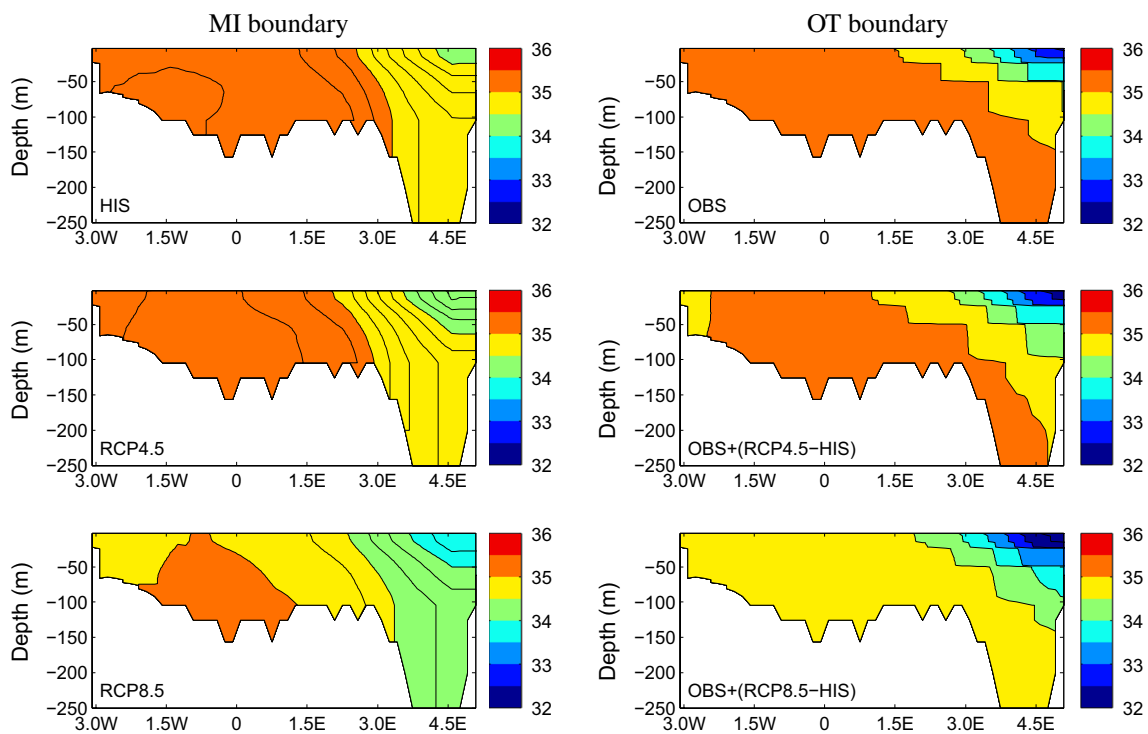


Fig. 10 30-year mean salinity over the historical period (1980–2009) and the future period (2071–2100) along the northern North Sea boundary (59.25°N). MI boundary: salinity is taken from EC-Earth including interannual variation. HIS, RCP4.5 and RCP8.5 represent the climatology from the historical and future simulations for the two sce-

narios, respectively. OT boundary: salinity is taken from observed climatology plus a freshening trend in the future ocean derived from EC-Earth. OBS represents the ICES observational climatology; The future period climatology is calculated by OBS plus the differences between RCPs and HIS climatology

References

- Ådlandsvik B (2008) Marine downscaling of a future climate scenario for the North Sea. *Tellus A* 60(3):451–458
- Ådlandsvik B, Bentsen M (2007) Downscaling a twentieth century global climate simulation to the North Sea. *Ocean Dyn* 57(4):453–466
- BACC (2011) Assessment of climate change for the Baltic Sea Basin. Springer, Berlin
- Berg P (2012) Mixing in HBM. DMI scientific report no. 12-03. Copenhagen, 21 pp. <http://www.dmi.dk/dmi/sr12-03>. ISSN: 978-87-7478-610-8
- Christensen J, Christensen O (2007) A summary of the PRUDENCE model projections of changes in European climate by the end of this century. *Clim Chang* 81:7–30
- Christensen O, Drews M, Christensen J, Dethloff K, Ketelsen K, Hebestadt I, Rinke A (2006) The HIRHAM regional atmospheric climate model version 5. DMI technical report 06-17, 22 pp. <http://www.dmi.dk/dmi/tr06-17>
- CMIP5 update (2010) Addendum to the CMIP5 experiment design document: a compendium of relevant emails sent to the modeling group. IPCC. http://cmip-pcmdi.llnl.gov/cmip5/docs/Experiment_design_addendum
- Dangendorf S, Wahl T, Hein H, Jensen J, Mai S, Mudersbach C (2012) Mean sea level variability and influence of the North Atlantic Oscillation on long-term trends in the German Bight. *Water* 4(1):170–195
- Dooley H (1974) Hypotheses concerning the circulation of the northern North Sea. *J du Conseil* 36(1):54–61
- Hazeleger W, Wang X, Severijns C, Ștefănescu S, Bintanja R, Sterl A, Wyser K, Semmler T, Yang S, Van den Hurk B et al (2012) EC-Earth V2. 2: description and validation of a new seamless earth system prediction model. *Clim Dyn* 39(11):2611–2629
- Hjøllø SS, Skogen MD, Svendsen E (2009) Exploring currents and heat within the North Sea using a numerical model. *J Mar Syst* 78(1):180–192
- Holt J, Wakelin S, Lowe J, Tinker J (2010) The potential impacts of climate change on the hydrography of the northwest European continental shelf. *Prog Oceanogr* 86(3):361–379
- Janssen F, Schrum C, Backhaus J (1999) A climatological data set of temperature and salinity for the Baltic Sea and the North Sea. *Dtsch Hydrogr Z* 51:5–245
- Jones J, Howarth M (1995) Salinity models of the southern North Sea. *Cont Shelf Res* 15(6):705–727
- Madsen K (2009) Recent and future climatic changes in temperature, salinity, and sea level of the North Sea and the Baltic Sea. Ph.D. thesis, University of Copenhagen
- Mathis M, Mayer B, Pohlmann T (2013) An uncoupled dynamical downscaling for the North Sea: method and evaluation. *Ocean Model* 72:153–166
- Meier H (2006) Baltic Sea climate in the late twenty-first century: a dynamical downscaling approach using two global models and two emission scenarios. *Clim Dyn* 27(1):39–68
- Orvik KA, Skagseth Ø (2005) Heat flux variations in the eastern Norwegian Atlantic Current toward the Arctic from moored instruments, 1995–2005. *Geophys Res Lett* 32:L14610
- Otto L, Zimmerman J, Furnes G, Mork M, Sætre R, Becker G (1990) Review of the physical oceanography of the North Sea. *J Sea Res* 26(2):161–238
- Stephenson D, Pavan V, Collins M, Junge M, Quadrelli R (2006) North Atlantic Oscillation response to transient greenhouse gas forcing and the impact on European winter climate: a CMIP2 multi-model assessment. *Clim Dyn* 27(4):401–420
- Svendsen E, Sætre R, Mork M (1991) Features of the northern North Sea circulation. *Cont Shelf Res* 11(5):493–508
- Taylor K, Stouffer R, Meehl G (2012) An overview of CMIP5 and the experiment design. *Bull Am Meteorol Soc* 93(4):485–498
- Tian T, Boberg F, Christensen O, Christensen J, She J, Vihma T (2013) Resolved complex coastlines and land–sea contrasts in a high-resolution regional climate model: a comparative study using prescribed and modelled SSTs. *Tellus A* 65. doi:10.3402/tellusa.v65i0.19951
- Tsimplis MN, Shaw AG (2008) The forcing of mean sea level variability around Europe. *Glob Planet Chang* 63(2):196–202
- Turrell W, Slesser G, Payne R, Adams R, Gillibrand P (1996) Hydrography of the East Shetland Basin in relation to decadal North Sea variability. *ICES J Mar Sci* 53(6):899–916
- Umlauf L, Burchard H, Hutter K (2003) Extending the $k - \omega$ turbulence model towards oceanic applications. *Ocean Model* 5(3):195–218
- van Vuuren D, Edmonds J, Kainuma M, Riahi K, Thomson A, Hibbard K, Hurtt G, Kram T, Krey V, Lamarque J et al (2011) The representative concentration pathways: an overview. *Clim Chang* 109:5–31
- Wakelin S, Holt J, Proctor R (2009) The influence of initial conditions and open boundary conditions on shelf circulation in a 3D ocean-shelf model of the North East Atlantic. *Ocean Dyn* 59(1):67–81
- Winther NG, Johannessen JA (2006) North Sea circulation: Atlantic inflow and its destination. *J Geophys Res* 111:C12018
- Yan Z, Tsimplis MN, Woolf D (2004) Analysis of the relationship between the North Atlantic oscillation and sea-level changes in northwest Europe. *Int J Climatol* 24(6):743–758